Available online at www.sciencedirect.com
ScienceDirect
Trans. Nonferrous Met. Soc. China 33(2023) 1361−1372
Transactions of Nonferrous Metals Society of China
www.tnmsc.cn

In-situ solid state repairing method for failure flat clinched joint of aluminum alloy

Peng ZHANG[1,2], Chao CHEN[3], Sheng-dun ZHAO[1],
Liang-yu FEI[1], Yang-feng CAO[1], Shuo-wen ZHANG[1], Xiao-lan HAN[4], Kun LI[1]

1. School of Mechanical Engineering, Xi'an Jiaotong University, Xi'an 710049, China;
2. College of Mechanical Engineering, Xi'an University of Science and Technology, Xi'an 710054, China;
3. State Key Laboratory of High Performance Complex Manufacturing, Light Alloy Research Institute, Central South University, Changsha 410083, China;
4. Mechanical Engineering College, Xi'an Shiyou University, Xi'an 710065, China

Received 13 December 2021; accepted 12 April 2022

Abstract: An in-situ solid state repairing method for the failure flat clinched joint was proposed to reconstruct the appearance and improve the mechanical properties. The microstructure, mechanical properties, and fracture failure behavior of the flat clinched and repaired joints were comparatively investigated to clarify feasibility and effectiveness of this method. Results indicate that the fractured neck of failure flat clinched joint is successfully repaired in-situ. The microstructure of the weld nugget is sufficiently refined, which enhances the mechanical properties of the repaired joint. Rotation speed and dwell time play crucial roles on the mechanical properties of joints. Compared with the initial flat clinched joint, the mechanical properties of the repaired joint are strengthened by the metallurgical bonding. The repaired joint has 409.90% higher maximum shear tension strength and 68.92% longer maximum extension at fracture. In addition, the fracture failure behaviors demonstrate that the repaired joint is much stronger than the flat clinched joint. This method for repairing the failure flat clinched joint is proven to be feasible and effective.

Key words: flat clinched joint; solid state repairing; average grain size; shear tension strength; fracture failure behavior

1 Introduction

Aluminum alloys are widely used in the aircraft, automotive, and construction industries for their environmental benefits, low density and high specific strength [1]. The flat clinching technology has been extensively employed in joining of the aluminum alloy sheets, according to GERSTMANN and AWISZUS [2] and CHEN et al [3]. This technology relies on the plastic deformation of the sheets to form a mechanical interlock and does not require the additional rivets, such as traditional riveting and self-pierce riveting (SPR) [4]. The shaping die is also substituted by a planar anvil, which avoids the formation of a protrusion at the bottom of the joint [5]. In contrast with resistance spot welding (RSW) and fusion welding, flat clinching exhibits many advantages, such as no spark, smoke, cracks, and porosity defects. Many researchers have investigated the mechanism of flat clinching [6], optimization of die geometry [7], especially mechanical properties and fracture failure behavior of the flat clinched joints [8]. However, studies on how to repair the failure flat clinched joints are scarce. If the damaged joints cannot be effectively repaired, then they will seriously affect the safety and function of the

Corresponding author: Sheng-dun ZHAO, E-mail: sdzhao@xjtu.edu.cn
DOI: 10.1016/S1003-6326(23)66188-6

structures in industry. This is a significant challenge in this field that requires immediate attention, and it has great practical importance.

According to KUMMA and SORANANSRI [9], the flat clinched joints typically experience shear tension damage during service, and neck fracture is the most common fracture mode [10]. The neck fractured joint cannot normally serve, due to the separation of the upper and lower sheets. Repairing the damaged neck using mechanical joining technologies is difficult. A special rivet is embedded into the keyhole of the failure clinched joint by SHI et al [11], CHEN et al [12], and REN et al [13]. Although the damaged mechanical interlock was rebuilt with the help of the rivet, the fractured neck was still not repaired. In addition, the use of rivet increases the mass and cost. Therefore, an in-situ repair method that can restore the original appearance of the joint and improve its mechanical properties is the most anticipated approach.

Friction stir welding (FSW) is a solid state joining method which is also often used to repair defects in metal structures [14]. HU et al [15] conducted a feasibility study on repairing defects of aircraft aluminum alloy structural parts, such as pore, crack, and gap, using the FSW method. REN et al [16] repaired the cracks in the aluminum alloy plate by using the FSW method, and the strength and ductility of the repaired specimen were basically equivalent to those of the base material. ZHANG et al [17] repaired the failure lap joints using the FSW method, and the fracture strength of the repaired joints was greatly improved for advancing side loading configuration. Friction stir spot welding (FSSW) is an evolution of FSW, which is also widely used for the repair of crack and void [18]. SAJED et al [19] repaired cracks and voids in the depth of thick aluminum plates via multilayer friction stir plug welding. The effects of tool rotation speed and dwell time on the mechanical properties were investigated by them. VENUKUMAR et al [20] repaired the keyhole defect of the FSSWed joints using a pinless FSSW tool. The repaired joint has stronger mechanical properties than the initial joint owing to the metallurgical bond between the filler plate and the surrounding material. Therefore, the FSSW method is expected to repair the failure flat clinched joints, and it allows a metallurgical bond to be formed at the fractured neck. The FSSWed and flat clinched joints have similar morphological appearance, with keyhole and plastic deformation zone (PDZ) observed on the upper surface. Furthermore, the flat bottom surface allows them to be used for visible areas and functional surfaces. Although YANG et al [21] and YAZDI et al [22] pointed out that the keyhole defects may affect the mechanical properties of the FSSWed joints, this is certainly considered a technical advantage in reconstructing the initial appearance of failure flat clinched joint.

Only if the repaired joint is stronger than the original flat clinched joint can it continue to serve better in the structures and equipment. BABU et al [23] investigated the effect of tool geometry and welding process parameters on the mechanical properties of the FSSWed joints. The obtained joints are found to be superior to riveted joints in shear tension and cross tension tests. FAHMY et al [24] concluded that the metallurgical bond and grain refinement make the shear tension strength of the FSSWed joint stronger than that of the RSWed joint. In view of its numerous technical advantages, FSSW is considered an alternative to traditional joining processes, such as SPR, RSW, fusion welding, and riveting [25,26]. Therefore, FSSW is a promising in-situ solid state repair method for failure flat clinched joints, and its feasibility and effectiveness are worthy of verification and investigation.

In industrial service, the appearance and mechanical properties of the joint are significant factor in evaluating the applicability and safety performance of the joint. The flat clinched joint will fail or crack when the shear tension load exceeds its ultimate shear tension strength. However, it is difficult to meet the service requirements by repairing the failure joint via mechanical joining methods. Therefore, the repair and strengthening method of the failure joints is particularly important. In this study, an in-situ repair method is proposed to reconstruct the appearance and improve the mechanical properties of the failure flat clinched joints using the FSSW technology. The innovation of this method is the in-situ solid state repair of the fractured neck. The feasibility and effectiveness of this method are demonstrated by comparing the microstructure, mechanical properties, and fracture failure behavior of the repaired joint with that of the initial flat clinched joint.

2 Experimental

2.1 Material

Commercial purity AA1100 was widely used in automotive power battery housings, battery busbars and decorative panels because of its good electrical and thermal conductivity, corrosion resistance, and forming properties. The spot joining of AA1100 has become a hot research topic in the field of advanced joining technology. In this study, 2 mm-thick AA1100 sheets with dimensions of 25 mm × 100 mm were used as base materials. Figure 1 shows the lath-like microstructure of this material with an average grain size of 22.19 μm. The chemical composition and mechanical properties of AA1100 are shown in Table 1 and Table 2, respectively.

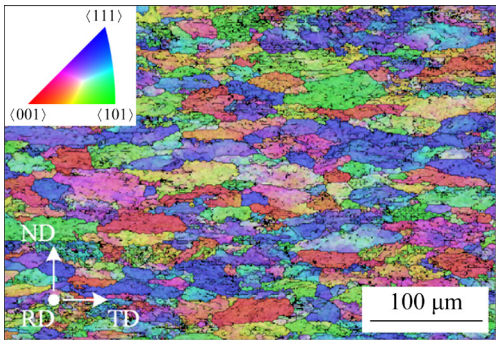

Fig. 1 Microstructure of AA1100 used in this study

Table 1 Chemical composition of AA1100 used in this study (wt.%)

Fe	Cu	Zn	Mn	Si	Al
0.54	0.1	0.015	0.05	0.05	Bal.

Table 2 Mechanical properties of AA1100 used in this study

Young's modulus/GPa	Tensile strength/MPa	Yield strength/MPa	Elongation/%
69	163.68	150.27	5

2.2 Flat clinching and damaging process

Flat clinching obtains a one-sided planar spot joint via a single forming process, and the principle is shown in Fig. 2(a). The mechanical interlocking is formed between the sheets relying on the plastic deformations of the sheets. The flat clinching tool typically consists of a flat die, punch, holder, and disc spring, as shown in Fig. 2(b). According to the previous geometrical optimization of flat clinching tools [7], the main geometrical dimensions of the tools used in this study are shown in Fig. 2(a): 2.75 mm punch radius (R) with 2° draft angle (α), 0.05 mm punch corner radius (r_p), and 5.95 mm holder radius (r). GERSTMANN and AWISZUS [2] and LÜDER et al [5] concluded that the mechanical properties of the flat clinched joint mainly depend on the bottom thickness (X), interlocking (t_s), and neck thickness (t_n). As shown in Fig. 2(b), the strong flat clinched joint with 0.5 mm of X, 0.18 mm of t_s and 0.38 mm of t_n was prepared on the Instron 5982 universal material testing machine (Instron 5982) as a base object.

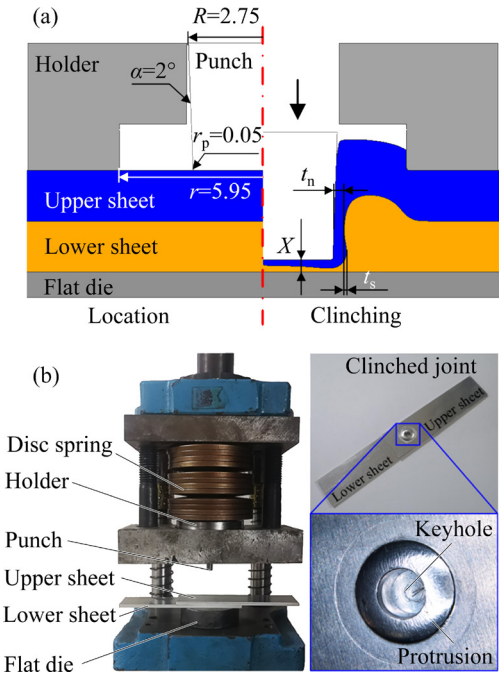

Fig. 2 Principle of flat clinching (a) and construction of flat clinching tool and clinched joint (b) (unit: mm)

According to LAMBIASE and DI ILID [27] and CHEN et al [10], the shear tension test was used to evaluate the mechanical properties of the flat clinched joint and imitate the damaging process. As shown in Fig. 3, the flat clinched joint was damaged before the repairing stage, which experienced neck fracture during the shear tension test, and the loading directions of shear tension loads (T) are demonstrated by the grey arrows.

2.3 Repairing process

Figure 4 illustrates the in-situ solid state repairing process of failure flat clinched joint. First, the damaged joint is rigidly clamped on the fixture, and the fractured neck needs to be aligned as much

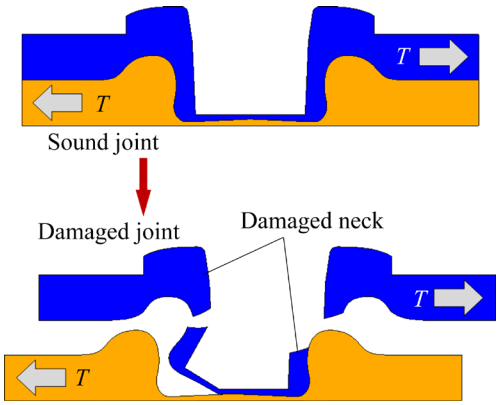

Fig. 3 Shear tension damaging of flat clinched joint

as possible to ensure a good repair quality. Thereafter, the rotating FSSW tool is plunge into the keyhole of the damaged joint until the tool shoulder reaches the setting plunge depth. Accordingly, a metallurgical bonding is formed around the keyhole after a certain period (dwell time) of friction and extrusion effect of the tool. As a result, the damaged joint is repaired in-situ after the tool retracts to the coordinate origin and stops rotating.

The repair experiments are carried out on the FSSW equipment, as shown in Fig. 5(a). Figure 5(b) shows the geometric characteristics of the FSSW tool made from H13 tool steel: 15 mm shoulder diameter with 1 mm concentric circle depth, 3.5 mm pin length with 1 mm thread pitch, and 6 mm pin root diameter with 15° draft angle (β). According to the studies on FSSW of commercial purity aluminum alloy by COLMENERO et al [28] and SENAPATI and BHOI [29], the used repairing parameters (i.e., rotation speed ω, dwell time t, plunge rate v, and plunge depth h) are listed in Table 3.

2.4 Mechanical properties test and transverse section observation

The feasibility of the repairing method is demonstrated by the visual and transverse section

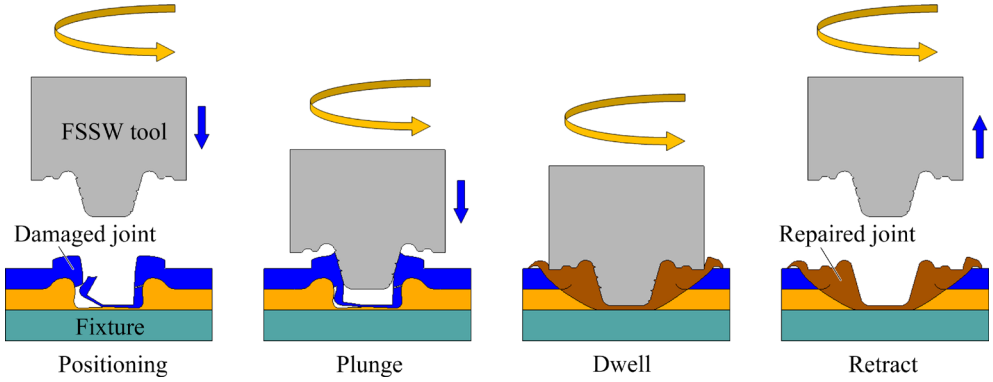

Fig. 4 Repairing process for damaged joint

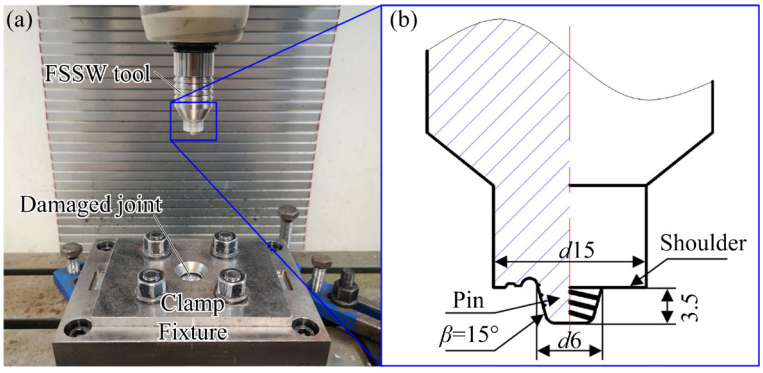

Fig. 5 FSSW equipment (a) and FSSW tool configuration and its dimensions (b) (unit: mm)

Table 3 Repairing parameters used in this study

ω/(r·min^{-1})	t/s	v/(mm·min^{-1})	h/mm
600, 800, 1000, 1200, 1400	2, 4, 6, 8, 10	10, 20, 30, 40, 50	0.1

observations, and the influences of repairing parameters on the mechanical properties and microstructures are also investigated. The metallographic specimens are prepared by cutting the transverse sections of the flat clinched and repaired joints along the diameter, perpendicular to the rolling direction of the AA1100 sheet. These sections are subjected to analysis of repairing effectiveness and microstructural distribution of the joints with Nikon SMZ745 stereomicroscope, optical microscope, and electron back scattered diffraction (EBSD) after mechanical grinding, polishing, and ion thinning.

After the repair, the shear tension strength of the repaired joints are conducted on the Instron 5982 based on the AWS D8.9M:2012 standard. The test method and specimen are shown in Fig. 6, and the loading directions of shear tension loads (T) are demonstrated by the grey arrows. The loading speed is 1 mm/min. The shear tension load represents an average of at least three joints to guarantee the accuracy of results. The fracture specimen is prepared by cutting transverse section of the fracture-failed joint along T, and the fracture behavior and mechanism are analyzed with Nikon SMZ745 stereomicroscope and Zeiss EVO MA 10 tungsten filament scanning electron microscope (SEM), respectively.

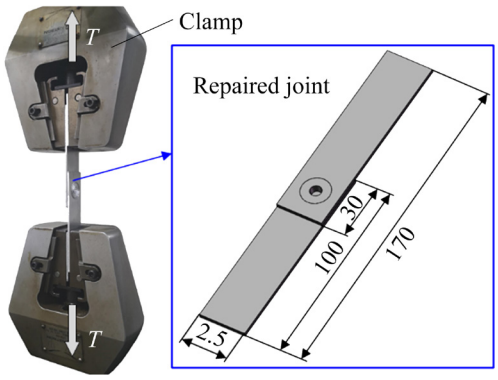

Fig. 6 Test method and specimen used for shear tension strength test (unit: mm)

3 Results and discussion

3.1 Macro- and micro-structure

The macroscopic appearance similarity between the repaired and the initial flat clinched joints is considered to be an important guarantee for the applicability of the joint. As shown in Fig. 7, the initial flat clinched and repaired joints share similar appearance characteristics. The keyhole and PDZ can be observed on the upper surface. Although the diameter of the latter is slightly larger than that of the former, this does not affect the practical application. SAJU et al [30] found that the diameter of the repaired joint can be reduced by changing the shoulder diameter of the FSSW tool, provided that the connection quality is guaranteed. The PDZ of the two joints is characterized by a protrusion on the upper surface based on the process principles. The height of the joint (H) is also another important parameter that determines the applicability of the joint, and the H of 4.2 mm of the repaired joint is less than the 4.3 mm of the flat clinched joint, as shown in Fig. 8.

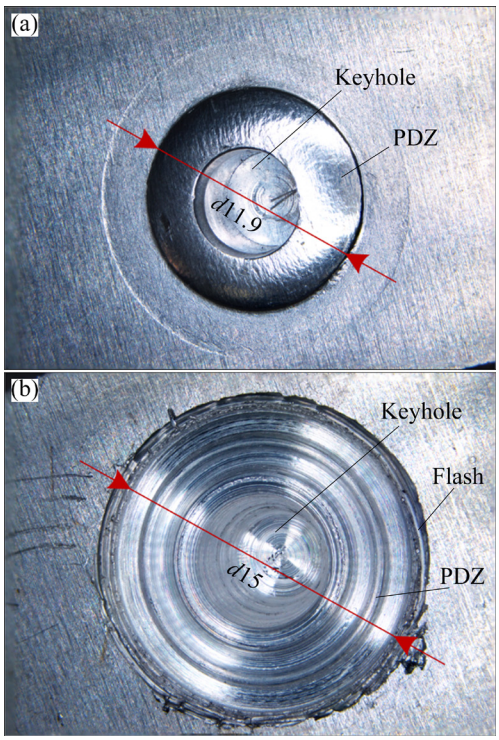

Fig. 7 Macroscopic appearance of joint: (a) Flat clinched joint; (b) Repaired joint (unit: mm)

Figure 8 illustrates the shear tension damaging of the flat clinched joint and the repair result of the damaged joint. The mechanical interlocking is formed to hook the upper and lower sheets in all of the 0.5 mm (X) flat clinched joints prepared in this study, as shown in Fig. 8(a). During shear tension damage, the joint neck will be fractured when T exceeds the permanent deformation limit, as shown in Fig. 8(b). The comparison between Figs. 8(b) and (c) shows that the damaged neck is successfully repaired in-situ. In contrast with the initial flat

clinched joint, a reliable metallurgical joining between the upper and lower sheets is formed in the repaired joint, with the interface gradually disappearing. Metallurgical joining is the most representative feature of the FSSWed joint with the support of YAZDI et al [22]. According to the microstructural characteristic of aluminum alloy, the transverse section of the repaired joint can be divided into four regions, namely, stir zone (SZ), thermo-mechanically affected zone (TMAZ), heat affected zone (HAZ), and base material (BM). The FSSWed joints obtained by BABU et al [23] and GARG and BHATTACHARYA [31] also show similar characteristics. Therefore, the macroscopic appearance and transverse section reveal that the FSSW method can be used to repair the failure flat clinched joint in-situ without compromising its appearance applicability.

Figure 9 shows the microstructures of four different regions (i.e., *A* to *D*) identified in Fig. 8. During flat clinching, the microstructure in the neck is elongated under the effect of plastic deformation, resulting in the formation of a number of fine grains. As shown in Fig. 9(a), the white arrow indicates the direction of grain deformation in Region A, with an average grain size of 7.34 μm. For the repaired joint, the material in the SZ experienced complete dynamic recrystallization phenomenon owing to severe welding heat and stir of the FSSW tool. The lath-like microstructure of AA1100 BM is sufficiently refined to a fine equiaxed grain structure in Region *B*, with an average grain size of 2.06 μm, as shown in Fig. 9(b). The effect of welding heat and plastic deformation on the TMAZ

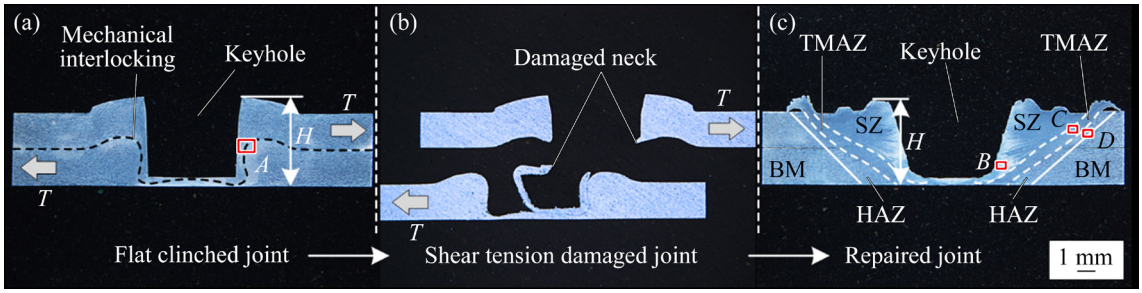

Fig. 8 Transverse section macrographs of joints: (a) Flat clinched joint; (b) Shear tension damaged joint; (c) Repaired joint

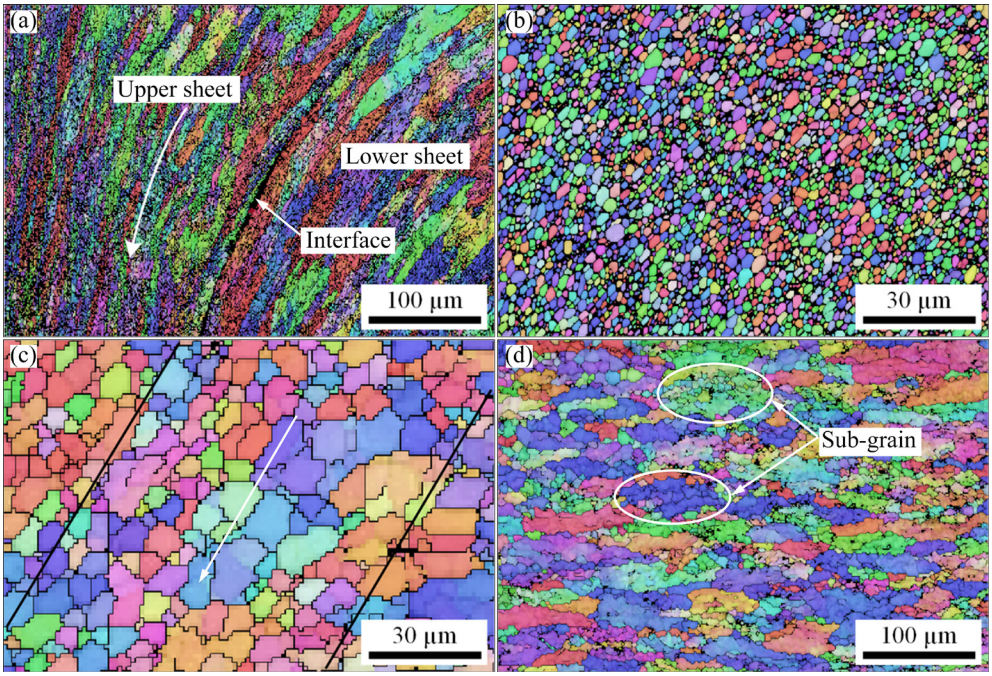

Fig. 9 Microstructures of Region *A* in Fig. 8 identified in flat clinched joint (a), and Regions *B*−*D* in Fig. 8 identified in repaired joint (b−d), respectively

is much lower than that on the SZ due to the location further away from the pin. Accordingly, the material in the TMAZ experienced partial recrystallization and recovery. The microstructure in Region *C* is elongated and distorted along the direction of the white arrow, with an average grain size of 6.81 μm, as shown in Fig. 9(c). By contrast, the material in the HAZ experienced recovery under welding heat without plastic deformation. The typical heat-grown microstructure with quasi-isometric sub-grains can be observed in Region *D*, and the average grain size is 11.18 μm, as shown in Fig. 9(d).

The mechanical properties of the repaired joint are directly determined by the microstructure, as stated by SENAPATI and BHOI [29]. The repairing parameters are the key factors for the welding heat input and plastic deformation that affect the grain size of the material. The microstructure and average grain size of the repaired joints at different rotation speeds are investigated. As shown in Fig. 10, the microstructures of the different zones of the joints repaired at varying rotation speeds have similar characteristics, with HAZ > TMAZ > SZ as the average grain size rank. The rising welding heat caused the grain to grow with the increase of the rotation speed, with the support of MAHMOUD and KHALIFA [32]. In contrast with Figs. 10(a) to (e), the boundaries of different zones appear progressively clear at 600−1000 r/min and suddenly become blurred. The average grain sizes of different zones are increased from 4.28 to 8.04 μm, 5.17 to 9.83 μm, and 9.81 to 11.36 μm, respectively, as shown in Fig. 10(f).

3.2 Shear tension strength

Figure 11 shows the shear tension results of the joints repaired under different welding parameters. They share the similar trend in that the shear tension loads rapidly increase to the maximum

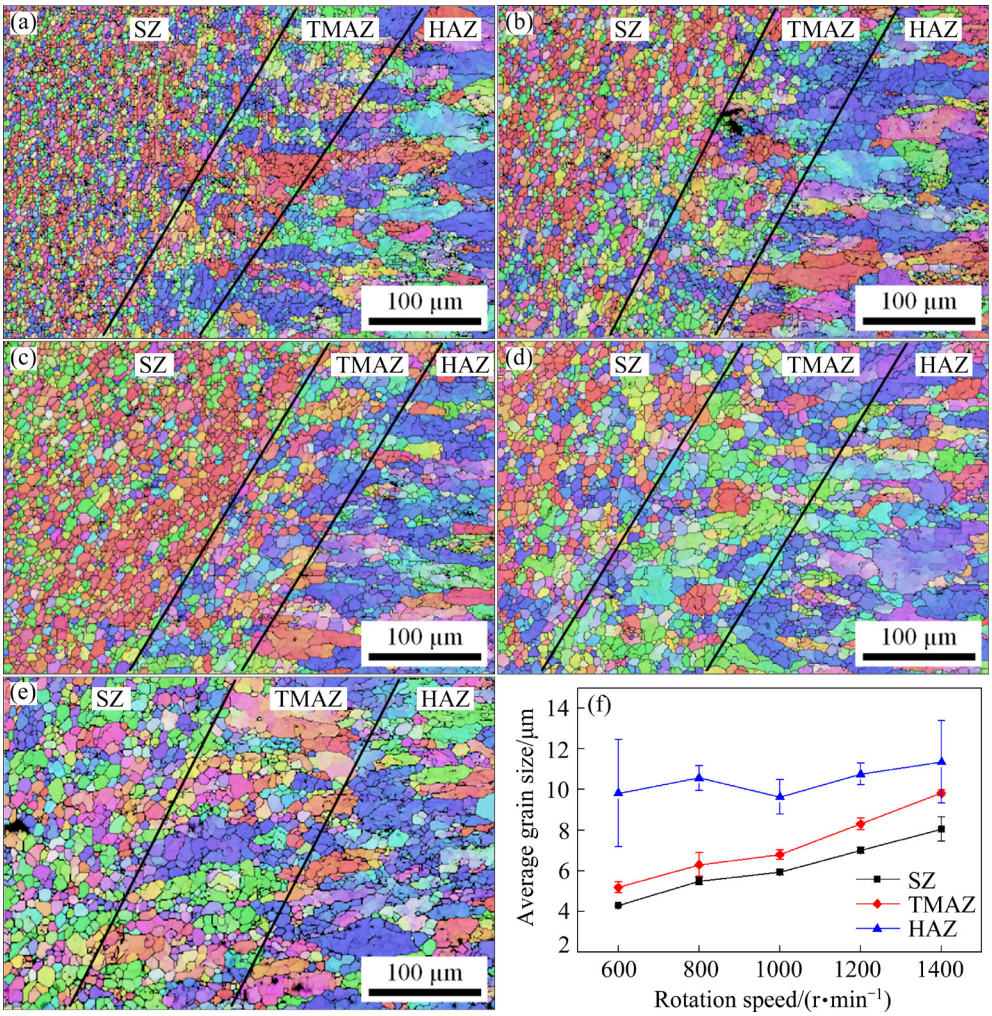

Fig. 10 Microstructure of different zones (a−e) and average grain size of repaired joints at different rotation speeds (f): (a) 600 r/min; (b) 800 r/min; (c) 1000 r/min; (d) 1200 r/min; (e) 1400 r/min

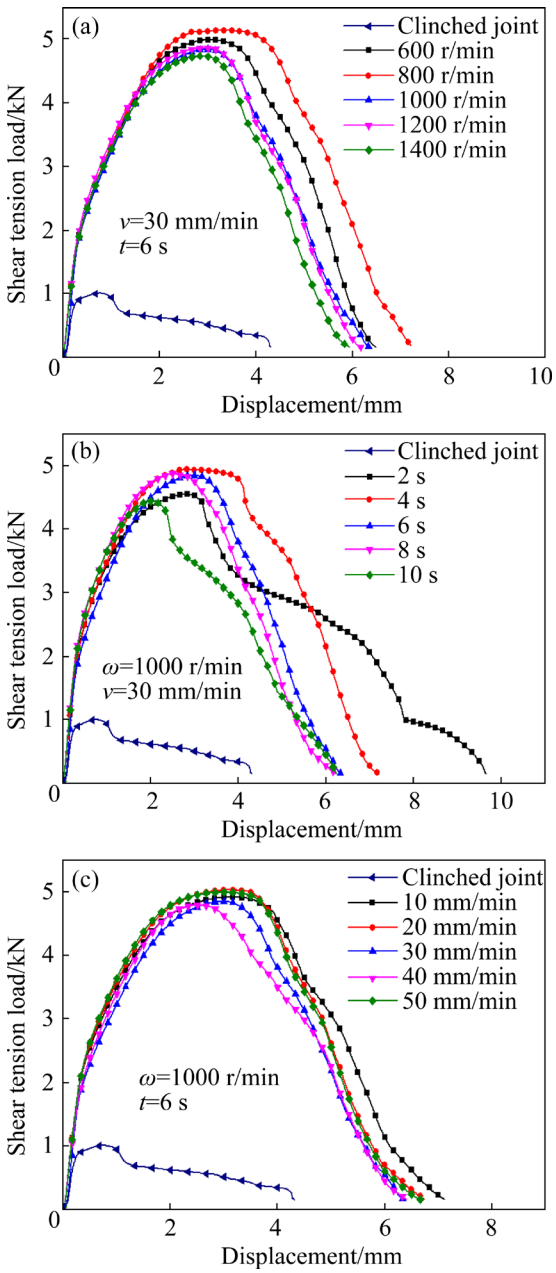

Fig. 11 Shear tension load−displacement curves of joints repaired under different welding parameters: (a) Rotation speed; (b) Dwell time; (c) Plunge rate

with displacement and gradually decrease to a minimum until the joint failure. In addition, the shear tension strength and extension at fracture are not significantly affected by the plunge rate, as shown in Fig. 11(c), which is consistent with the findings of CHU et al [33]. By contrast, the shear tension load−displacement curve of the flat clinched joint presents much lower shear tension strength and extension at fracture than the repaired joints, as shown in Fig. 11. The maximum shear tension load and maximum extension at fracture of the repaired joint (ω=800 r/min, t=6 s, and v=30 mm/min) are 5.15 kN and 7.23 mm, while the flat clinched joint are 1.01 kN and 4.28 mm, respectively. Therefore, the repaired joint has a 409.90% higher maximum shear tension load and 68.92% longer maximum extension at fracture.

Figure 12 shows that the maximum shear tension loads of the repaired joints change with rotation speed and dwell time. AA1100 is a type of non-heat treatable reinforced aluminum alloy, the welding heat may cause the grain to grow and reduce its mechanical properties, as investigated by ABNAR et al [34]. Accordingly, the average maximum shear tension load of the repaired joints decreases with the rotation speed and dwell time increasing, except that the joints are repaired at 600 r/min and 2 s, respectively. These results are consistent with those of SENAPATI and BHOI [29] and PRABHA et al [35]. When the damaged joint is repaired at a short dwell time of 2 s or a slow rotation speed of 600 r/min, the amount of welding heat input is not sufficient to soften the BM and simultaneously weld them. The weak welding and void defects are observed in the joint, as shown in Fig. 13.

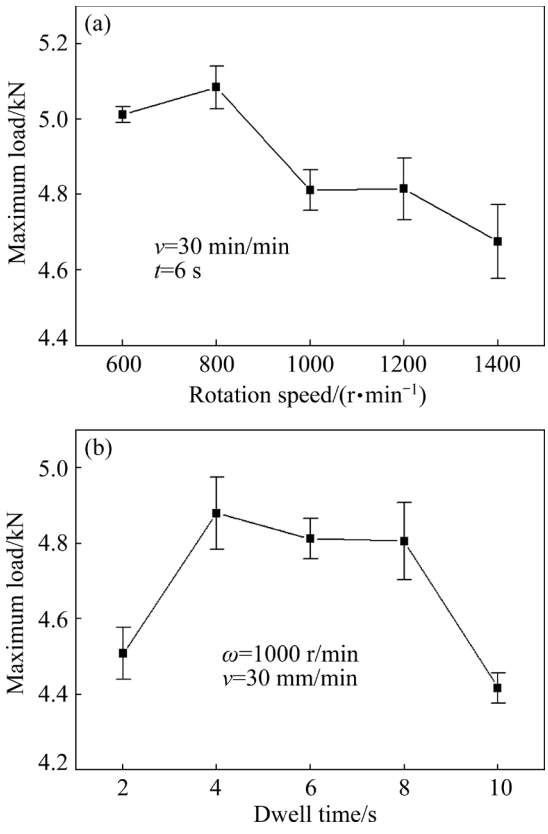

Fig. 12 Maximum load of joint repaired under different welding parameters: (a) Rotation speed; (b) Dwell time

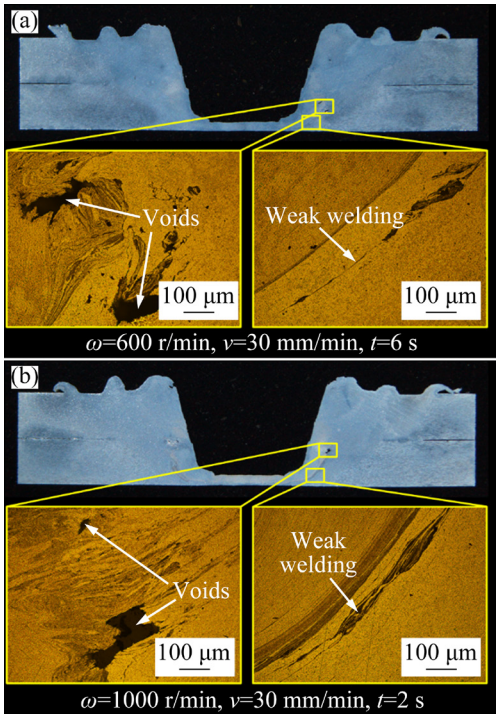

Fig. 13 Weak welding and void defects of joints repaired at different parameters: (a) Slow rotation speed; (b) Short dwell time

3.3 Fracture modes under shear tension loading

According to the experimental results, all the repaired joints fracture in the BM and HAZ/TMAZ boundary under shear tension loading. The fracture mode is not significantly affected by the repairing parameters. The transverse sections and fracture appearances of the fracture-failed joints are analyzed to compare the fracture mode of the flat clinched and repaired joints. In this research, the fracture mode for all of the flat clinched joints is the neck fracture mode, as shown in Fig. 14(a). The neck is fractured under the shear tension because the shear tension resistance of mechanical interlocking is stronger than that of the neck. In addition, the button is twisted due to the good ductility of the AA1100, consistent with the findings of CHEN et al [3]. During the shear tension test, the weld nugget of the repaired joint is twisted to ensure that the loads T acting on the two sheets are collinear. The comparison of the transverse sections shows that the metallurgical bonding area of the repaired joint is much larger than the mechanical interlocking of the flat clinched joint. Therefore, the shear tension strength of the repaired joint is much stronger than that of the flat clinched joint. The repaired joint exhibits a hybrid failure mode of the neck and upper sheet tensile fracture while the SZ basically remains intact, as shown in Fig. 14(b).

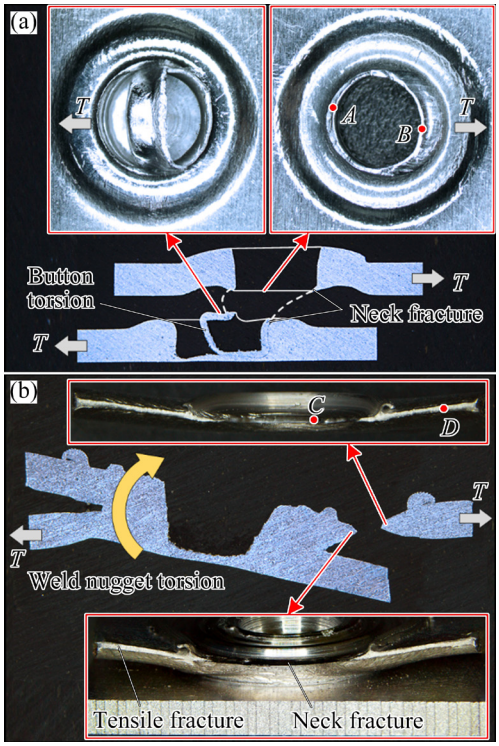

Fig. 14 Shear tension fracture mode of joints: (a) Flat clinched joint; (b) Repaired joint

Figure 15 shows the shear tension fracture surface morphologies of two joints at different regions (i.e., A−D) identified in Fig. 14. During the shear tension damage, the shear stress is subjected on the neck as a dominant force. The typical quasi-parabolic shear dimples can be observed in the neck fracture region of the flat clinched joint, as shown in Figs. 15(a) and (b). The opening of the parabola is consistent with the shear stress. The tensile stress acted on the rear side of the shear fracture is more significant than on the front side due to the button twisting, hence, its shear dimples are much deeper. After the in-situ repair, metallurgical joining is formed between the upper and lower sheets and the fractured neck. The SZ and TMAZ of the repaired joint carry the shear tension loads during shear tension test. The initial crack at the sheet interface propagated along the HAZ/TMAZ boundary and finally through the upper sheet. Consequently, the flat shear dimples can be observed in the neck fracture region due to the shear and torsional action of the shear and

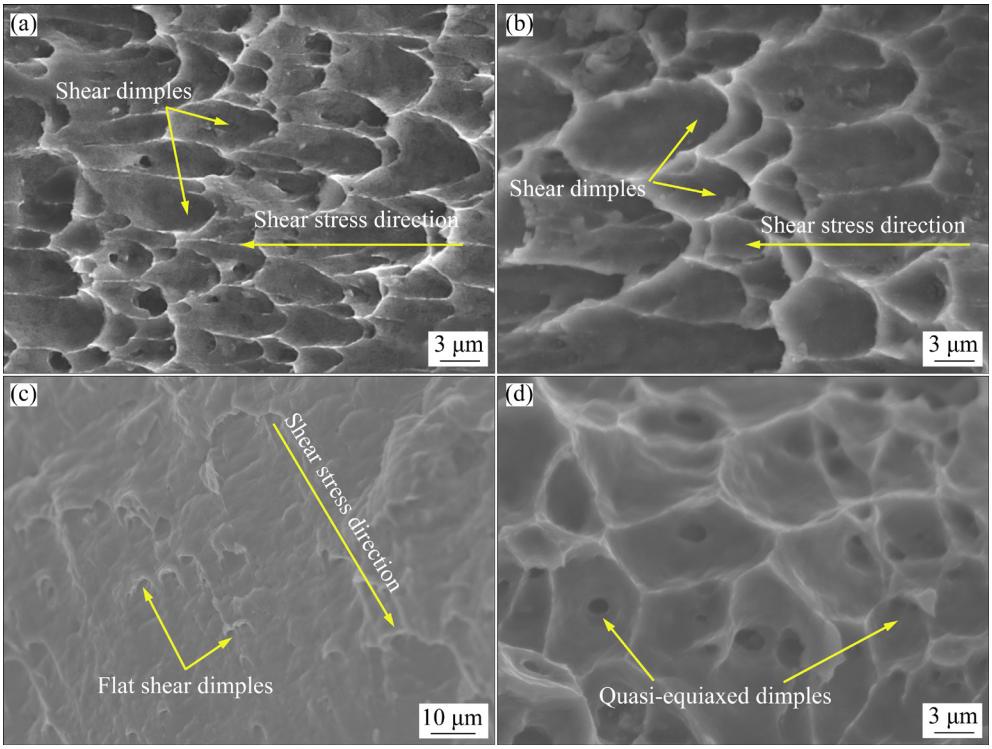

Fig. 15 Shear tension fracture surface morphologies of flat clinched (a, b) and repaired (c, d) joint of Regions *A*−*D* in Fig. 14, respectively

tensile stresses on the joint, as shown in Fig. 15(c). Tensile fracture takes place at the upper sheet, which is characterized by typical quasi-equiaxed dimples, because the weld nugget is stronger than the BM, as shown in Fig. 15(d).

In this research, the failure flat clinched joint is successfully in-situ repaired using the proposed repairing method. The experimental results prove that the FSSW is an effective and promising method to repair the neck fractured joint without affecting its practical application. In addition, the proposed in-situ repairing method can be further used to repair the failure joints, such as riveted, RSWed, and SPRed joints, which are difficult to be reconnected using the initial process. This method is considered to be more suitable for joints of lightweight and plastic materials, such as aluminum alloys, magnesium alloys, copper, and mild steel.

The shear tension strength of the repaired joint is stronger than that of the initial flat clinched joint, which benefits from the metallurgical joining. However, the welding heat input must be controlled to reduce its effect on the mechanical properties during the repairing of non-heat treatable reinforced aluminum alloy joint.

Furthermore, the influence of the alignment of fracture neck on the repair quality must be investigated in the future work, which will be helpful to enhancing the usefulness and convenience of the proposed in-situ repairing method.

4 Conclusions

(1) The mechanical interlocking of the flat clinched joint exhibit neck fracture when it bears high shear tension load. After repair, the mechanical interlocking is replaced by a metallurgical bond. The plastic deformation zone diameter and protrusion height of the repaired joint do not differ much from those of the flat clinched joint, thereby guaranteeing the practical application of the joint.

(2) The microstructures of SZ, TMAZ, and HAZ are sufficiently refined compared with BM, and the average grain sizes are 2.06, 6.81, and 11.18 μm, respectively. The average grain size in different regions grow with the increase of the rotation speed. When the rotation speed is over 1000 r/min, the excessive welding heat causes the grain to severely grow and reduce the mechanical properties.

(3) The mechanical properties of the repaired joint are strengthened by the metallurgical bond

between the upper and lower sheets and the fractured neck compared with the initial flat clinched joint. The repaired joint has a 409.90% higher maximum shear tension strength and 68.92% longer maximum extension at fracture.

(4) The fracture failure behaviors demonstrate that the repaired joint is much stronger than the flat clinched joint. The flat clinched joint exhibits neck fracture failure mode. Meanwhile, the repaired joint exhibits a hybrid failure mode of neck and upper sheet tensile fracture, and its SZ basically remains intact.

Acknowledgments

This research was financially supported by the National Natural Science Foundation of China (Nos. 51675414, 51805416), and the Joint Fund for Aerospace Advanced Manufacturing Technology Research Key Program, China (No. U1937203).

References

[1] XU Wei-feng, MA Jun, WANG Miao, LU Hong-jian, LUO Yu-xuan. Effect of cooling conditions on corrosion resistance of friction stir welded 2219-T62 aluminum alloy thick plate joint [J]. Transactions of Nonferrous Metals Society of China, 2020, 30(6): 1491−1499.

[2] GERSTMANN T, AWISZUS B. Hybrid joining: Numerical process development of flat-clinch-bonding [J]. Journal of Materials Processing Technology, 2020, 277: 116421.

[3] CHEN Chao, ZHANG Hui-yang, REN Xiao-qiang, WU Jin-liang. Investigation of flat-clinching process using various thicknesses aluminum alloy sheets [J]. The International Journal of Advanced Manufacturing Technology, 2021, 114(7): 2075−2084.

[4] ABE Y, MAEDA T, YOSHIOKA D, MORI K. Mechanical clinching and self-pierce riveting of thin three sheets of 5000 series aluminium alloy and 980 MPa grade cold rolled ultra-high strength steel [J]. Materials, 2020, 13(21): 4741.

[5] LÜDER S, HÄRTEL S, BINOTSCH C, AWISZUS B. Influence of the moisture content on flat-clinch connection of wood materials and aluminium [J]. Journal of Materials Processing Technology, 2014, 214(10): 2069−2074.

[6] PENG Hao, CHEN Chao, ZHANG Hui-yang, RAN Xiang-kun. Recent development of improved clinching process [J]. The International Journal of Advanced Manufacturing Technology, 2020, 110(11): 3169−3199.

[7] HAN Xiao-lan, ZHAO Sheng-dun, CHEN Chao, LIU Chen, XU Fan. Optimization of geometrical design of clinching tools in flat-clinching [J]. Proceedings of the Institution of Mechanical Engineers, Part C: Journal of Mechanical Engineering Science, 2017, 231(21): 4012−4021.

[8] CHEN Chao, ZHANG Hui-yang, XU Yong-qian, WU Jin-liang. Investigation of the flat-clinching process for joining three-layer sheets on thin-walled structures [J]. Thin-Walled Structures, 2020, 157: 107034.

[9] KUMMA P, SORANANSRI P. Effect of blank holder force and edge radius on joining strength in flat-clinching process [J]. Key Engineering Materials, 2020, 856: 175−181.

[10] CHEN Chao, ZHANG Hui-yang, ZHAO Sheng-dun, REN Xiao-qiang. Effects of sheet thickness and material on the mechanical properties of flat clinched joint [J]. Frontiers of Mechanical Engineering, 2021, 16(2): 410−419.

[11] SHI Chen, YI Rui-xiang, CHEN Chao, PENG Hao, RAN Xiang-kun, ZHAO Sheng-dun. Forming mechanism of the repairing process on clinched joint [J]. Journal of Manufacturing Processes, 2020, 50: 329−335.

[12] CHEN Chao, RAN Xiang-kun, PAN Qing, ZHANG Hui-yang, YI Rui-xiang, HAN Xiao-lan. Research on the mechanical properties of repaired clinched joints with different forces [J]. Thin-Walled Structures, 2020, 152: 106752.

[13] REN Xiao-qiang, CHEN Chao, RAN Xiang-kun, LI Yu-xiang, ZHANG Xin-gang. Microstructure evolution of AA5052 joint failure process and mechanical performance after reconditioning with tubular rivet [J]. Transactions of Nonferrous Metals Society of China, 2021, 31(11): 3380−3393.

[14] MEHTA K P, PATEL R, VYAS H, MEMON S, VILAÇA P. Repairing of exit-hole in dissimilar Al−Mg friction stir welding: Process and microstructural pattern [J]. Manufacturing Letters, 2020, 23: 67−70.

[15] HU Jin, DING Li-li, GUO Bi-xin, FANG Wen-peng. Technical research of friction stir welding repair in aeroplane aluminium alloy damage [J]. Advanced Materials Research, 2010, 154/155: 1262−1265.

[16] REN Jun-Gang, WANG Lei, XU Dao-Kui, XIE Li-Yang, ZHANG Zhan-Chang. Analysis and modeling of friction stir processing-based crack repairing in 2024 aluminum alloy [J]. Acta Metallurgica Sinica (English Letters), 2017, 30(3): 228−237.

[17] ZHANG Hui-jie, LIU Xu, LIU Hui-jie, MEI Rui-bin, CHEN Xiao-guang. Interfacial feature and mechanical property of friction stir lap repair welded 7B04 aluminum alloy [J]. Journal of Materials Engineering and Performance, 2020, 29(10): 6890−6897.

[18] KÖHLER T, YU C N, SCHMIDT K, GRÄTZEL M, WU Yang-yang, BERGMANN J, SEKULIC D, JEAN P, BERGMANN. Development of a repair process for manmade structures in space by using aluminium brazing and friction stir spot welding [J]. Welding Technology Review, 2019, 91(9): 39−50.

[19] SAJED M, HOSSEIN SEYEDKASHI S M. Multilayer friction stir plug welding: A novel solid-state method to repair cracks and voids in thick aluminum plates [J]. CIRP Journal of Manufacturing Science and Technology, 2020, 31: 467−477.

[20] VENUKUMAR S, YALAGI S G, MUTHUKUMARAN S, KAILAS S V. Static shear strength and fatigue life of refill friction stir spot welded AA 6061-T6 sheets [J]. Science and Technology of Welding and Joining, 2014, 19(3): 214−223.

[21] YANG Xia-wei, FENG Wu-yuan, LI Wen-ya, DONG Xiu-rong, XU Ya-xin, CHU Qiang, YAO Shuo-tian.

Microstructure and properties of probeless friction stir spot welding of AZ31 magnesium alloy joints [J]. Transactions of Nonferrous Metals Society of China, 2019, 29(11): 2300−2309.

[22] YAZDI S R, BEIDOKHTI B, HADDAD-SABZEVAR M. Pinless tool for FSSW of AA 6061-T6 aluminum alloy [J]. Journal of Materials Processing Technology, 2019, 267: 44−51.

[23] BABU S, SANKAR V S, JANAKI RAM G D, VENKITAKRISHNAN P V, REDDY G M, RAO K P. Microstructures and mechanical properties of friction stir spot welded aluminum alloy AA2014 [J]. Journal of Materials Engineering and Performance, 2013, 22(1): 71−84.

[24] FAHMY M H, ABDEL-ALEEM H, ELKOUSY M R, ABDEL-ELRAHEEM N M. Comparative study of spot welding and friction stir spot welding of Al 2024-T3 [J]. Key Engineering Materials, 2018, 786: 104−118.

[25] MUBIAYI M P, AKINLABI E T, MAKHATHA M E. Current state of friction stir spot welding between aluminium and copper [J]. Materials Today: Proceedings, 2018, 5(9, Part 3): 18633−18640.

[26] REIMANN M, GOEBEL J, DOS SANTOS J F. Microstructure and mechanical properties of keyhole repair welds in AA 7075-T651 using refill friction stir spot welding [J]. Materials & Design, 2017, 132: 283−294.

[27] LAMBIASE F, DI ILIO A. Damage analysis in mechanical clinching: Experimental and numerical study [J]. Journal of Materials Processing Technology, 2016, 230: 109−120.

[28] COLMENERO A N, OROZCO M S, MACÍAS E J, FERNÁNDEZ J B, MURO J C S D, FALS H C, ROCA A S. Optimization of friction stir spot welding process parameters for Al−Cu dissimilar joints using the energy of the vibration signals [J]. The International Journal of Advanced Manufacturing Technology, 2019, 100(9): 2795−2802.

[29] SENAPATI N P, BHOI R K. Improving the strength of friction-stir-welded joints of AA1100 alloy [J]. Journal of Materials Engineering and Performance, 2021, 30(1): 510−521.

[30] SAJU T P, NARAYANAN R G, ROY B S. Effect of pinless tool shoulder diameter on dieless friction stir extrusion joining of AA 5052-H32 and AA 6061-T6 aluminum alloy sheets [J]. Journal of Mechanical Science and Technology, 2019, 33(8): 3981−3997.

[31] GARG A, BHATTACHARYA A. Similar and dissimilar joining of AA6061-T6 and copper by single and multi-spot friction stirring [J]. Journal of Materials Processing Technology, 2017, 250: 330−344.

[32] MAHMOUD T S, KHALIFA T A. Microstructural and mechanical characteristics of aluminum alloy AA5754 friction stir spot welds [J]. Journal of Materials Engineering and Performance, 2014, 23(3): 898−905.

[33] CHU Qiang, YANG Xia-wei, LI Wen-ya, LI Yong-bing. Microstructure and mechanical behaviour of pinless friction stir spot welded AA2198 joints [J]. Science and Technology of Welding and Joining, 2016, 21: 164−170.

[34] ABNAR B, KAZEMINEZHAD M, KOKABI A H. Effects of heat input in friction stir welding on microstructure and mechanical properties of AA3003-H18 plates [J]. Transactions of Nonferrous Metals Society of China, 2015, 25(7): 2147−2155.

[35] PRABHA K A, PUTHA P K, PRASAD B S. Effect of tool rotational speed on mechanical properties of aluminium alloy 5083 weldments in friction stir welding [J]. Materials Today: Proceedings, 2018, 5(9, Part 3): 18535−18543.

失效铝合金平底无铆连接接头的原位固相修复方法

张 鹏[1,2]，陈 超[3]，赵升吨[1]，费亮瑜[1]，曹杨峰[1]，张硕文[1]，韩晓兰[4]，李 坤[1]

1. 西安交通大学 机械工程学院，西安 710049；
2. 西安科技大学 机械工程学院，西安 710054；
3. 中南大学 轻合金研究院，高性能复杂制造国家重点实验室，长沙 410083；
4. 西安石油大学 机械工程学院，西安 710065

摘 要：为了修复失效平底无铆连接接头并提高其力学性能，提出一种原位固相修复方法。通过对比研究平底无铆连接接头和修复接头的显微组织、力学性能和断裂失效行为，验证修复方法的可行性和有效性。结果表明，失效平底无铆连接接头的断裂颈部被成功地原位修复。焊核的显微组织被充分细化，使得修复接头的力学性能得到提升。转速和持续加热时间对修复接头的力学性能起着至关重要的作用。与平底无铆连接接头相比，冶金结合使修复接头的力学性能得到加强。修复接头的最大拉剪强度提高了 409.90%，最大断裂伸长量提高了 68.92%。断裂失效行为表明，修复接头的强度明显高于原始平底无铆连接接头，这说明失效平底无铆连接接头的修复方法是可行有效的。

关键词：平底无铆连接；固相修复；平均晶粒尺寸；拉剪强度；断裂失效行为

(Edited by Xiang-qun LI)